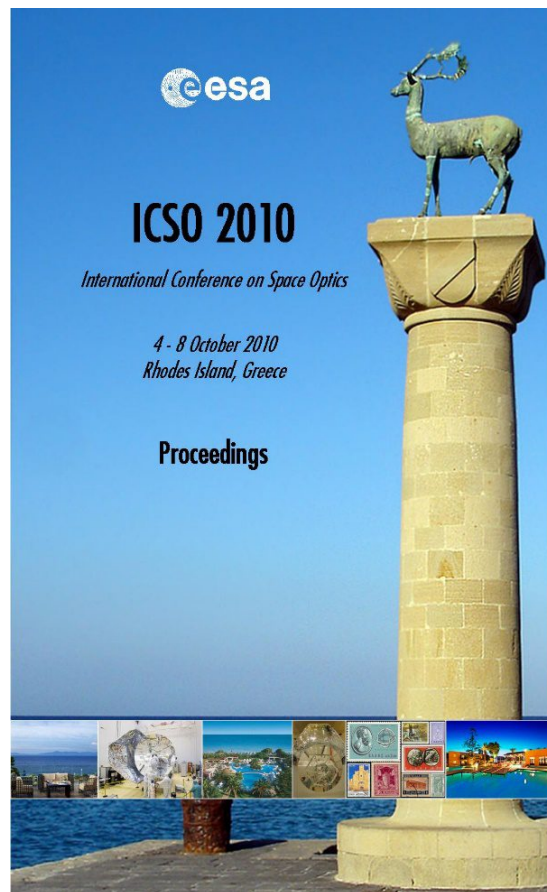


International Conference on Space Optics—ICSO 2010

Rhodes Island, Greece

4–8 October 2010

*Edited by Errico Armandillo, Bruno Cugny,
and Nikos Karafolas*



Parameter design and experimental study of a bifunctional isolator for optical payload protection and stabilization

*Guang-yuan Wang, Xin Guan, Dong-jing Cao,
Shao-fan Tang, et al.*



International Conference on Space Optics — ICSO 2010, edited by Errico Armandillo, Bruno Cugny,
Nikos Karafolas, Proc. of SPIE Vol. 10565, 105651P · © 2010 ESA and CNES
CCC code: 0277-786X/17/\$18 · doi: 10.1117/12.2309098

PARAMETER DESIGN AND EXPERIMENTAL STUDY OF A BIFUNCTIONAL ISOLATOR FOR OPTICAL PAYLOAD PROTECTION AND STABILIZATION

Wang Guang-yuan¹, Guan Xin¹, Cao Dong-jing², Tang Shao-fan², Chen Xiang², Liang Lu¹, Zheng Gang-tie¹
¹ School of Aerospace, Tsinghua University, China. ² Beijing Institute of Space Mechanics & Electricity, China

Contact Details

Mailing Address: School of Aerospace, Tsinghua University, Beijing, 100084, China

Email: wang-gy08@mails.tsinghua.edu.cn

I. INTRODUCTION

With the raise of resolution, optical payloads are becoming increasingly sensitive to satellite jitter. An approach where the entire spacecraft is pointed with great accuracy requires sophisticated and expensive bus design. In an effort to lower the overall cost of space missions that require highly stable line-of-sight pointing, a method of separating the bus and the payload with low frequency isolators is proposed. This isolation system can block the transmission of disturbance and allow relatively large bus motion. However, if the isolator is linear then there is a trade-off between isolation and static deflection as the launch and the on-orbit stage have difference requirements on the isolation frequency. Otherwise, an extra locking system should be appended to protect the payload before getting into orbit, as the STABLE isolation system^[1] and the MIM isolation system^[2] did.

To overcome this limitation, an alternative approach is to design a nonlinear isolator with high-static stiffness during launch and low dynamic stiffness on orbit. Several specially designed nonlinear isolators have achieved low dynamic stiffness with large static load capacity. Virgin^[3] considered a structure made from a highly deformed elastic element to achieve a softening spring. Platus^[4] exploited the buckling of beams under axial load in a specific configuration to achieve a negative stiffness in combination with a positive stiffness, and hence low-dynamic stiffness. Others have achieved the same by connecting linear springs with positive stiffness in parallel with elements of negative stiffness^{[5]-[7]}.

In the present study, a bifunctional isolator has been developed for optical payloads. The isolator have good performance both during launch and on orbit because of its specially designed nonlinear stiffness and damping. The isolator works in a linear part with low stiffness and small damping ratio under the micro-vibration and microgravity on orbit. The transmissibility requirement and the displacement restriction during launch are satisfied by tuning the nonlinear stiffness and damping parameters. A group of sample isolators are designed tested both statically and dynamically.

II. MECHANICAL MODEL DESIGN

The dynamic environment during launch is quite different from on-orbit. In the launch phase, the overload factor varies slowly and can be treated as quasi-static load. Meanwhile, large dynamic load is induced by jet vibration, noise, and stage separation. When the spacecraft get into orbit, the quasi-static load disappears and the vibration induced by the moving parts on the satellite is at the micro level. A nonlinear isolator can be constructed with different equivalent stiffness under the two load conditions to meet the different requirements of these two phases. The equivalent stiffness under launch load should be high enough to restrict the static deformation, while the on-orbit state stiffness should be much lower to isolate the disturbing vibration. According to the requirements, a mechanical model possessing low stiffness when the deformation is small and higher stiffness when the deformation is large can be constructed, as is shown in Fig.1.

Assuming the static load is F_s and expanding the nonlinear stiffness as exponential series, the stiffness of the isolator can be expressed as

$$\tilde{f}_k(x) = \begin{cases} -\sum_{i=1}^{\infty} a_i (x-x_1)^i + f_1 & x \leq x_1 \\ k_0(x-x_1) + f_1 & x_1 < x \leq x_2 \\ \sum_{i=1}^{\infty} a_i (x-x_2)^i + f_2 & x > x_2 \end{cases} \quad (1)$$

where

$$f_2 = k_0(x_2 - x_1) + f_1 \quad (2)$$

The static load

$$F_s = \frac{f_1 + f_2}{2} \quad (3)$$

The damping force can be written as

$$\tilde{f}_c(\dot{x}, x) = \begin{cases} c_1 \dot{x} & x \leq x_1 \\ c_0 \dot{x} & x_1 < x \leq x_2 \\ c_1 \dot{x} & x > x_2 \end{cases} \quad (4)$$

The width of linear part is define as

$$\Delta x = x_2 - x_1 \quad (5)$$

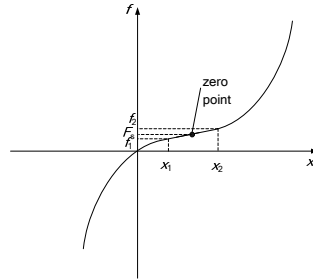


Fig. 1. Stiffness Curve of the Isolator

III. DYNAMIC RESPONSE ANALYSIS

A. On-orbit Transmissibility

The on-orbit excitation at the payload mounting surface is typically low level wide band micro vibration, with the spectrum distributing from 5Hz to 2000Hz. By setting the width of linear part larger than the maximum relative displacement of the payload, the isolator will work in the linear part on orbit. Therefore, the on-orbit isolation frequency is solitarly determined by k_0

$$f_0 = \frac{1}{2\pi} \sqrt{\frac{k_0}{m}} \quad (6)$$

According to the classical vibration isolation theory, the isolation frequency should be less than $1/\sqrt{2}$ times of the lower bound of the disturbing frequency. To achieve better isolation performance, the isolation frequency should be lower and the damping ratio should not be too large. Typically, the isolation frequency is no less than 1Hz to avoid coupling with the attitude control system.

B. Launch Transmissibility

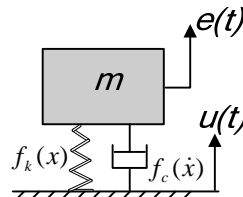


Fig. 2. Single Degree of Freedom System

During launch, the spacecraft endures large quasi-static load and severe dynamic load. The stiffness of the isolator should be high enough to restrict the displacement of the payload. In addition, the isolation frequency should be tuned to avoid coupling vibration with the vehicle or the satellite. Since the natural frequency of the payload is usually much higher than the isolation frequency, the dynamic model can be simplified as a single degree of freedom system as shown in Fig.2.

By assuming the payload mass m , the displacement of the payload and the mounting surface $e(t)$ and $u(t)$, the governing equation can be written as

$$m\ddot{e} + f_k(e - u) + f_c(\dot{e} - \dot{u}, e - u) = F_s \quad (7)$$

Several methods for calculating the dynamic response of piecewise linear system are proposed in references [8]~[10], including harmonic balance method, equivalent linearization method, and perturbation method. However, there are limited research on the dynamic response of polynomial piecewise nonlinear system as shown in Fig. 1. In the present study, it is solved by applying harmonic balance method. Assuming the relative displacement

$$x = e - u \quad (8)$$

The equivalent dynamic equation can be written as

$$m\ddot{x}_d + c_{eq}\dot{x}_d + k_{eq}x_d = mB \sin \omega t \quad (9)$$

where B is the amplitude of the base acceleration and x_d is the dynamic component of the relative displacement. Assuming the response is harmonic

$$x_d(t) = A \sin(\omega t) \quad (10)$$

the equivalent stiffness k_{eq} and the equivalent damping c_{eq} can be expressed as^[11]

$$k_{eq} = \frac{1}{\pi A} \int_0^{2\pi} d\varphi \tilde{f}_k(A \sin \varphi) \sin \varphi \quad (11)$$

$$c_{eq} = \frac{1}{\pi \omega A} \int_0^{2\pi} d\varphi \tilde{f}_c(\omega A \cos \varphi, A \sin \varphi) \cos \varphi \quad (12)$$

Without loss of generality, one can specify that $x_1, x_2 > 0$. Expanding the integrand in (11) and (12), after a little algebra, one can obtain

$$k_{eq} = k_{eq}^{(1)} \Big|_0^{\theta_1} + k_{eq}^{(1)} \Big|_{\pi-\theta_1}^{2\pi} + k_{eq}^{(2)} \Big|_{\theta_1}^{\theta_2} + k_{eq}^{(2)} \Big|_{\pi-\theta_2}^{\pi-\theta_1} + k_{eq}^{(3)} \Big|_{\theta_2}^{\pi-\theta_2} \quad (13)$$

$$c_{eq} = c_{eq}^{(1)} \Big|_0^{\theta_1} + c_{eq}^{(1)} \Big|_{\pi-\theta_1}^{2\pi} + c_{eq}^{(2)} \Big|_{\theta_1}^{\theta_2} + c_{eq}^{(2)} \Big|_{\pi-\theta_2}^{\pi-\theta_1} + c_{eq}^{(3)} \Big|_{\theta_2}^{\pi-\theta_2} \quad (14)$$

where

$$\theta_1 = \begin{cases} \sin^{-1}\left(\frac{x_1}{A}\right) & A > x_1 \\ \frac{\pi}{2} & A \leq x_1 \end{cases} \quad (15)$$

$$\theta_2 = \begin{cases} \sin^{-1}\left(\frac{x_2}{A}\right) & A > x_2 \\ \frac{\pi}{2} & A \leq x_2 \end{cases} \quad (16)$$

$$k_{eq}^{(1)} = \frac{1}{\pi A} \left(\sum_{i=1}^n \sum_{k=0}^i a_i A^i C_i^k (-\sin \theta_1)^k S_{ik} - f_1 \cos \varphi \right) \quad (17)$$

$$k_{eq}^{(3)} = \frac{1}{\pi A} \left(\sum_{i=1}^n \sum_{k=0}^i b_i A^i C_i^k (-\sin \theta_2)^k S_{ik} - f_2 \cos \varphi \right) \quad (18)$$

$$k_{eq}^{(2)} = \frac{1}{\pi A} \left[kA \left(\frac{\varphi}{2} - \frac{1}{4} \sin 2\varphi \right) + kA \sin \theta_1 \cos \varphi - f_1 \cos \varphi \right] \quad (19)$$

$$c_{eq}^{(1)} = \frac{1}{\pi \omega A} \sum_{i=1}^n d_i \omega^i A^i G_i \quad (20)$$

$$c_{eq}^{(2)} = \frac{1}{\pi} c_0 \left(\frac{\varphi}{2} + \frac{1}{4} \sin 2\varphi \right) \quad (21)$$

$$c_{eq}^{(3)} = \frac{1}{\pi \omega A} \sum_{i=1}^n e_i \omega^i A^i G_i \quad (22)$$

$$S_{ij} = \int (\sin \varphi)^{i-j+1} d\varphi \quad (23)$$

$$G_i = \int \cos^{i+1} \varphi d\varphi \quad (24)$$

The absolute transmissibility can be written as

$$\Lambda_a(\omega) = \frac{k_{eq} + ic_{eq}\omega}{k_{eq} - m\omega^2 + ic_{eq}\omega} \quad (25)$$

The backbone equation is

$$k_{eq} - m\omega^2 = 0 \quad (26)$$

Equation (25) and (26) are implicit functions of the amplitude and frequency, which can be solved with Newton iteration method.

IV. PARAMETER DISCUSSION

To simplify the discussion of parameters, the stiffness of the nonlinear part is approximated with only one parameter by assuming

$$a_i = 0 \quad i \geq 2 \quad (27)$$

Define the second isolation frequency as

$$f_2 = \frac{1}{2\pi} \sqrt{\frac{a_1}{m}} \quad (28)$$

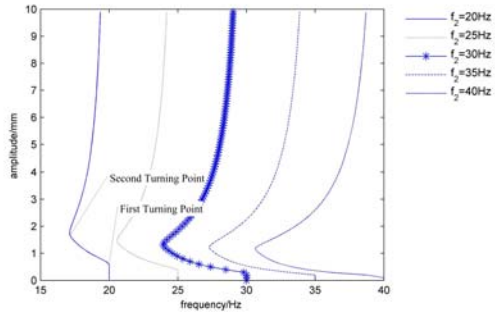


Fig. 3. Influence of Second Isolation Frequency on Backbone Curve

To examine the effect of the second isolation frequency alone, five different values of frequency 20, 25, 30, 35 and 40 are used here along with the assumption of both the width and the stiffness of the linear part are constant. Fig.3 illustrates its influence on the backbone curve.

Each curve in the figure has two turning points due to the characteristic of nonlinearity. When the amplitude increases, the deformation of the isolator becomes larger than x_1 and get into the linear part, where the equivalent stiffness, as well as the peak frequency, drops down and the first turning point appears. When the amplitude is large enough, the isolator pass through the linear part and get into the nonlinear part on the other side. Thus, the equivalent stiffness and the peak frequency rise and here comes the second turning point. The maximum excursion of the isolation frequency is the subtraction of the frequencies at the two turning points. Numerical results show that the excursion is magnified by the increase of the second isolation frequency.

The influence of the width of linear part on the transmissibility is examined by setting the second isolation frequency and the linear stiffness constant and choosing different value of Δx from 0.1mm to 2.5mm, as shown in Fig.4. It can be seen from the figure that all the curves share the same first turning point, and the amplitude of the second turning point is Δx larger than the first one. The bigger the width is, the larger the frequency excursion will be.

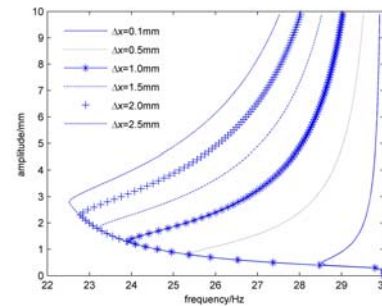


Fig. 4. Influence of Linear Width on Backbone Curve

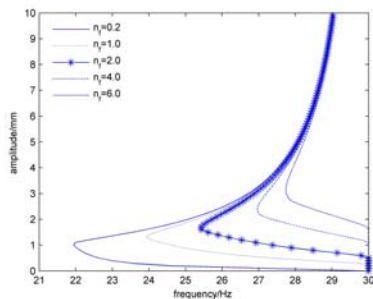


Fig. 5. Influence of Load Factor on Backbone Curve

Since the load factor varies during the launch phase, it is necessary to discuss its influence on frequency excursion. A bunch of curves are obtained with the load factor varying from 0.2 to 6.0 and all the other parameters being constant, as is shown in Fig.5. It can be deduced from the findings displayed in this figure that the frequency excursion is significantly enlarged when the load factor goes down. Accordingly, the isolation frequency should be examined with the lowest load factor to satisfy the frequency restriction.

The damping is another factor that significantly affects the isolation performance and needs proper design. As analyzed in section 3.1, the damping ratio of the linear part should be small to obtain acceptable on-orbit isolation performance. The effect of the damping coefficients of the nonlinear part is examined by assuming the linear part non-damped and all other parameters constant. It can be concluded from Fig.6 that the peak value drops down along the backbone curve as a result of an increase in the damping coefficient.

V. DESIGN APPROACH

The design problem for minimizing the vibration transmitted to the payload during launch can be formulated as the following optimization problem

$$\min e_{rms}(a_i, k_0, c_1, c_2, \Delta x) \quad (29)$$

subject to on-orbit isolation frequency constraint

$$[\omega_0]^l \leq \sqrt{k_0 / m} \leq [\omega_0]^u \quad (30)$$

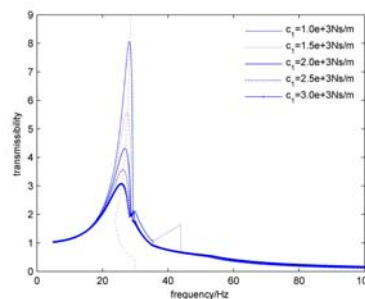


Fig. 6. Influence of Damping Coefficients on Transmissibility

Width constraint of linear part

$$\Delta x \geq [\Delta x]^l \quad (31)$$

Isolation frequency constraint during launch

$$[\omega]^l \leq \omega_{peak} \leq [\omega]^u \quad (32)$$

Peak value constraint of transmissibility during launch

$$\Lambda_a(\omega) \leq [\Lambda]^u \quad (33)$$

Static displacement constraint during launch

$$d(n_f) \leq [d]^u \quad (34)$$

Table 1 Design constraints and optimized parameters of the sample isolator

item	constraint	Design parameter	value
On-orbit isolation frequency f_0	1.5Hz	f_0	1.5Hz
Width of linear part Δx	>1mm	Δx	1mm
Isolation frequency during launch	20-35Hz	f_2	32Hz
Peak value of transmissibility during launch	<3.5	c_0	0Ns/m
Static displacement during launch	<3mm	c_1	2.5×10^3 Ns/m

The constraint equations defining the feasible domain are highly nonlinear in terms of the designing parameters. To overcome difficulties due to these nonlinearities, the multi-island genetic algorithm is applied to solve the problem. A sample isolator for 40kg payload is designed with this method. The design constraints and optimized parameters are listed in table 1.

VI. EXPERIMENTAL STUDY

A. Static Stiffness Test

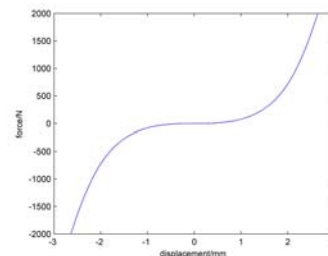


Fig. 7. Sample of the Isolator and Clamps for Static Test **Fig. 8.** Static Stiffness Curve of the Isolator

The sample isolators are manufactured according to the optimized parameters in section 5. Static test is conducted to verify the parameters, as is shown in Fig.7. Fig.8 is the tested static stiffness curve. With piecewise linear approximation and least square approximation approach, the tested parameters can be obtained as follows, $\Delta x = 0.92\text{mm}$, $f_0 = 1.50\text{Hz}$, $f_2 = 33.06\text{Hz}$. The width and stiffness of the linear part are quite close to the designed value, while the second isolation frequency is slightly higher but still within the constrained frequency range. The deformation of the isolator is 2.64mm when the load factor is 5.0, which means the isolator can effectively restrict the payload and avoid large amplitude sway during launch.

B. Launch Environment Test

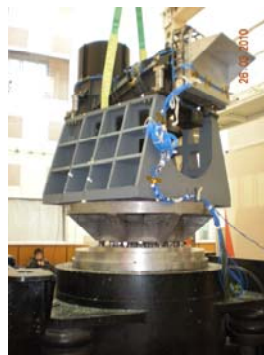


Fig. 9. Launch Environment Test

The launch environment test is conducted to verify the isolation performance during launch. The payload is connected to the vibration bracket by four isolators and excited from the bottom by the shaking table, as is shown in Fig.9. The power spectrum density of excitation and response is shown in Fig.10. From the tested transmissibility, it can be found that the peak frequency is 32.5Hz and the peak value is 3.29. The response

drops below the excitation level in the frequency range above 50Hz. The root mean square acceleration transmitted to the payload is attenuated to 28.82% of the excitation level, from which it can be concluded that the dynamic environment of the payload is well improved.

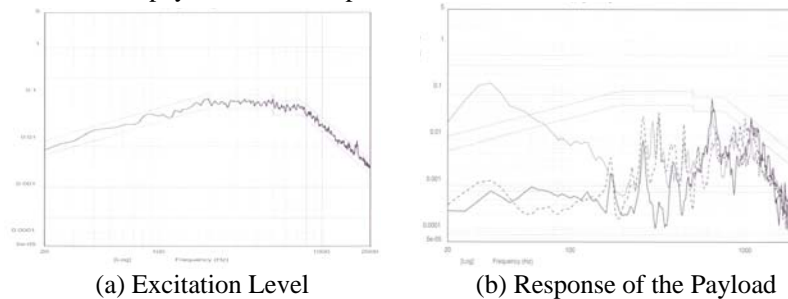


Fig. 10. Results of Launch Environment Test

VII. CONCLUSION

A bifunctional isolator with nonlinear stiffness and damping has been developed in the present study. The nonlinear characteristic is designed with a high stiffness under the launch load resulting in a small-static deflection, and a small dynamic stiffness on orbit resulting in a low natural frequency and hence a greater frequency range over which there is vibration isolation.

Influence of the parameters on the dynamic response during launch and on-orbit isolation performance is discussed. The major findings are as follows:

- a) Since the width of the linear part is larger than the maximum on-orbit relative amplitude, the isolation frequency is solitarily determined by the linear stiffness.
- b) Parameter study of the backbone curve shows that the isolation frequency excurses downward from the second isolation frequency when the excitation level rises. The excursion is positively related with the second isolation frequency and the width of the linear part while negatively related with the static load.
- c) It can be concluded from the transmissibility analysis that the peak point drops down along the backbone curve when the damping coefficient increases.

The optimization problem was formed to get the minimum vibration transmission design and solved by applying multi-island genetic algorithm. A group of sample isolators are manufactured based on the optimized parameters and tested statically and dynamically. Test results indicate that:

- a) The displacement of the isolator under the maximum static load is small, which means the payload can be effectively restricted during launch.
- b) The vibration transmitted to the payload was attenuated by more than 70%. So that the dynamic environment during launch is well improved.

REFERENCES

- [1] Edberg Donald L, Boucher Robert, Nurre Gerald S, Whorton Mark S. "Performance assessment of the STABLE Microgravity Vibration Isolation Flight Demonstration," *AIAA/ASME/ASCE/AHS/ASC Structures, Structural Dynamics, and Materials Conference and Exhibit*. USA: Kissimmee, FL, 7-10 April 1997.
- [2] Grodinsky Carlos M, Whorton Mark S. "Survey of Active Vibration Isolation Systems for Microgravity Applications," *Journal Of Spacecraft And Rockets*, vol.37, pp. 586-596, 2000.
- [3] Virgin L N, Santillan S T, Plaut R H. "Vibration isolation using extreme geometric nonlinearity," *Journal of Sound and Vibration*, vol. 315, pp. 721-731, 2008.
- [4] Platus D L. "Negative-stiffness-mechanism vibration isolation systems," *Proceedings of SPIE, Vibration Control in Microelectronics, Optics, and Metrology*. USA: Denver, CO, 21 July 1999.
- [5] Woodard S E, Housner J M. "Nonlinear behavior of a passive zero spring-rate suspension system," *Journal of Guidance, Control, and Dynamics*, vol. 14, pp. 84-89, 1991.
- [6] Alabuzhev P, Gritchin A., Kim L, Migirenko G, Chon V, Stepanov P. "Vibration Protecting and Measuring Systems with Quasi-Zero Stiffness". New York : Hemisphere Publishing Corporation, 1989.
- [7] Carrella A, Brennan M J, Waters T P. "Static analysis of a quasi-zero-stiffness vibration isolator," *Journal of Sound and Vibration*, vol. 301, pp. 678-689, 2007.
- [8] Iwan W D. "Generalization of the concept of equivalent linearization," *International Journal of Non-Linear Mechanics*, vol. 8, pp. 279-287, August 1973.
- [9] Natsiavas S, Gonzalez H. "Vibration of harmonically excited oscillators with asymmetric constrains," *Journal of Applied Mechanics*, vol. 59, pp. 284-290, 1992.
- [10] Narimani A., Golnaraghi M E, Jazar G N. "Frequency response of a piecewise linear vibration isolator," *Journal of Vibration and Control*, vol. 10, pp. 1775-1794, 2004.
- [11] Worden K, Tomlinson G R. "Nonlinearity in Structural Dynamics". Bristol: Institute of Physics Publishing, 2001.